

Free vibration analysis of a piezoelectric nanobeam using nonlocal elasticity theory

Abbas Kaghazian^a, Ali Hajnayeb* and Hamidreza Foruzande^a

Department of Mechanical Engineering, Faculty of Engineering, Shahid Chamran University of Ahvaz, Ahvaz, Iran

(Received March 24, 2016, Revised October 5, 2016, Accepted October 28, 2016)

Abstract. Piezoelectric nanobeams are used in several nano electromechanical systems. The first step in designing these systems is conducting a vibration analysis. In this research, the free vibration of a piezoelectric nanobeam is analyzed by using the nonlocal elasticity theory. The nanobeam is modeled based on Euler-Bernoulli beam theory. Hamilton's principle is used to derive the equations of motion and also the boundary conditions of the system. The obtained equations of motion are solved by using both Galerkin and the Differential Quadrature (DQ) methods. The clamped-clamped and cantilever boundary conditions are analyzed and the effects of the applied voltage and nonlocal parameter on the natural frequencies and mode shapes are studied. The results show the success of Galerkin method in determining the natural frequencies. The results also show the influence of the nonlocal parameter on the natural frequencies. Increasing a positive voltage decreases the natural frequencies, while increasing a negative voltage increases them. It is also concluded that for the clamped parts of the beam and also other parts that encounter higher values of stress during free vibrations of the beam, anti-nodes in voltage mode shapes are observed. On the contrary, in the parts of the beam that the values of the induced stress are low, the values of the amplitude of the voltage mode shape are not significant. The obtained results and especially the mode shapes can be used in future studies on the forced vibrations of piezoelectric nanobeams based on Galerkin method.

Keywords: free vibrations; piezoelectric; nonlocal elasticity; nanobeam

1. Introduction

In recent years, smart materials have been widely used in industries. Smart materials are materials that their material properties are affected by external electrical, thermal or magnetic fields. One of the most important types of smart materials is piezoelectric material (Song and Sethi and Li 2006).

Piezoelectric materials generate electrical voltage under mechanical stress, and deform if an electrical field is applied. Because of this unique property, they can be used in fabricating different types of sensors such as microphones, accelerometers and etc. They can also be used as actuators in resonators, micro mirrors, micro pumps and etc (Junwu and Zhigang and TaiJiang and Guangming and Boda 2005, Koh and Kobayashi and Hsiao and Lee 2010, Manzanque *et al.* 2014).

The theoretical studies on the modeling of piezoelectric materials has also been growing as fast as their extensive applications. There are numerous studies on the piezoelectric vibration control (Jalili 2009), actuation (Uchino 1997 and Zamanian and Khadem 2009), sensing (Gautschi 2002) and energy harvesting (Erturk and Inman 2011). Recently, a new and different branch in the theory of piezoelectricity has been introduced after using these

materials in miniaturized systems. This branch is based on the nonlocal elasticity theory that considers the small size effects.

In nano scale, piezoelectric properties are modified by the size effects (Zhang and Wang 2012). Therefore, the nonlocal elasticity theory has been used for modeling piezoelectric nanobeams, recently. Ke *et al.* (2012) studied the free vibrations of a piezoelectric nanobeam under different values of temperature, voltage and axial force. Ke *et al.* (2012), in a similar research, applied nonlocal elasticity and Timoshenko beam theory in order to study the nonlinear free vibrations of a piezoelectric nanobeam. In both studies, the natural frequencies and mode shapes of the nanobeam were obtained in different conditions using differential quadrature (DQ) method without any verification with other theories. Hosseini-Hashemi *et al.* (2014) studied the free vibrations of a functionally graded material (FGM) nanobeam. Because of the simplicity of the system, an analytical solution for the natural frequencies and mode shapes were found. In summary, in previous research works on the natural frequencies and mode shapes of a piezoelectric nanobeam based on nonlocal elasticity, mostly the DQ method was used, and there is no verification on the results. Conducting no verification could led to errors (for instance in (Ke and Wang 2012) that will be discussed, later). Thereby, a comparison study is necessary to verify the accuracy of the obtained characteristics of piezoelectric nanobeams with the nonlocal elasticity theory.

In this paper, the free vibration of a nanobeam is studied using the nonlocal elasticity theory. First, Hamilton's

*Corresponding author, Assistant Professor
E-mail: a.nayeb@scu.ac.ir

^aM.Sc.



Fig. 1 A schematic view of the nanobeam

principle is used to derive the governing equations and boundary conditions of the system. Subsequently, the resulting equations are solved using Galerkin method and also DQ method. Both vibration and voltage mode shapes and also the natural frequencies are obtained, and the effects of change in the nonlocal parameter and the applied voltage are studied. Finally, a comparison study is conducted between the results of DQ and Galerkin methods.

2. Theoretical modeling

The studied piezoelectric nanobeam is illustrated in Figure 1. The length and the thickness of the beam are L and h , respectively. The poling direction of the piezoelectric beam is the same as the direction of z -axis. An external voltage, V_0 , is applied between the upper and lower surfaces of the beam.

According to Euler-Bernoulli beam theory, the displacement components of an arbitrary point located on (x, z) of the nanobeam are given by

$$u(x, z, t) = U_n(x, t) - z \left(\frac{\partial W(x, t)}{\partial x} \right) \quad (1)$$

$$w(x, z, t) = W(x, t)$$

where $u(x, z, t)$ and $W(x, z, t)$ are the axial and transverse displacements, respectively. $U_n(x, t)$ is the axial displacement of a point on the beam neutral axis, and $W(x, t)$ is its transverse displacement. The axial strain component is

$$\varepsilon_{xx} = \frac{\partial U_n}{\partial x} - z \frac{\partial^2 W}{\partial x^2} = -z \frac{\partial^2 W}{\partial x^2}. \quad (2)$$

The second term in Eq. (2) is eliminated since the nonlinear mid-plane stretching component is neglected in the linear model of this study. The total electric potential function has to be in a form that satisfies the Maxwell equation. Therefore, it is considered as (Wang 2002a)

$$\Phi(x, z, t) = -\cos(\beta z) \phi(x, t) + \frac{zV_0}{h} \quad (3)$$

where $\beta = \frac{\pi}{h}$ and $\phi(x, z)$ is the electric potential. The components of the electric field are obtained through differentiating Eq. (3).

$$\begin{aligned} E_x &= -\frac{\partial \Phi}{\partial x} = \cos(\beta z) \frac{\partial \phi}{\partial x} \\ E_z &= -\frac{\partial \Phi}{\partial z} = \beta \sin(\beta z) \phi - \frac{V_0}{h} \end{aligned} \quad (4)$$

On the other hand, from nonlocal elasticity theory, the fundamental equations of piezoelectric materials are (Ke and Wang 2012)

$$\begin{aligned} \sigma_{ij} - (e_0 a)^2 \nabla^2 \sigma_{ij} &= C_{ijkl} \varepsilon_{kl} - e_{kij} E_k \\ D_i - (e_0 a)^2 \nabla^2 D_i &= e_{ikl} \varepsilon_{kl} + \dot{d}_k E_k \end{aligned} \quad (5)$$

Where σ_{ij} , ε_{kl} , D_i , and E_k are stress, strain, electrical displacement and electrical field components, respectively. C_{ijkl} , e_{kij} and ε_{ik} are elastic, piezoelectric and dielectric constants, respectively. $e_0 a$ is the nonlocal parameter that is measured through experiments. Because of small thickness and width to length ratios of the nanobeam, Eq. (5) can be rewritten as

$$\sigma_{xx} - (e_0 a)^2 \frac{\partial^2 \sigma_{xx}}{\partial x^2} = C_{11} \varepsilon_{xx} - e_{31} E_z \quad (6)$$

$$D_x - (e_0 a)^2 \frac{\partial^2 D_x}{\partial x^2} = \dot{d}_1 E_x \quad (7)$$

$$D_z - (e_0 a)^2 \frac{\partial^2 D_z}{\partial z^2} = e_{31} \varepsilon_{xx} + \dot{d}_3 E_z \quad (8)$$

At this point, Hamilton's principle can be implemented:

$$\int_0^t \delta(U + W_F - T) dt = 0 \quad (9)$$

Where U , T and W_F are strain energy, kinetic energy and total work of the external forces.

The strain energy of the piezoelectric nanobeam is

$$U = \frac{1}{2} \int_0^L \int_{-\frac{h}{2}}^{\frac{h}{2}} (\sigma_{xx} \varepsilon_{xx} - D_x E_x - D_z E_z) dz dx \quad (10)$$

Substituting Eqs. (2) and (4) in Eq. (10) results in

$$\begin{aligned} U &= \frac{1}{2} \int_0^L [-M \frac{\partial^2 W}{\partial x^2} + \int_{-\frac{h}{2}}^{\frac{h}{2}} [-D_x \cos(\beta z) \frac{\partial \phi}{\partial x} dz + \\ &D_z (\beta \sin(\beta z) \phi + \frac{V_0}{h})] dx \end{aligned} \quad (11)$$

Where M is the bending moment and is defined as

$$M = \int_{-\frac{h}{2}}^{\frac{h}{2}} (\sigma_{xx} z) dz \quad (12)$$

The kinetic energy, T , and the work of the external forces, W_F , can be obtained from

$$T = \frac{1}{2} \int_0^L \rho A \left(\frac{\partial W}{\partial t} \right)^2 dx \quad (13)$$

And

$$W_F = \frac{1}{2} \int_0^L N_e \left(\frac{\partial W}{\partial x} \right)^2 dx \quad (14)$$

In Eq. (14), N_e is the applied external force. In this study, it is caused by applying an external voltage and can be found from the following equation.

$$N_e = \int_{-\frac{h}{2}}^{\frac{h}{2}} [e_{31} E_z] dz = -e_{31} v_0 \quad (15)$$

After substituting Eqs. (11), (13) and (14) into Eq. (9) and equating the coefficients of δW and $\delta \phi$ to zero, the governing equations can be obtained as

$$\frac{\partial^2 M}{\partial x^2} + N_e \frac{\partial^2 W}{\partial x^2} = \rho A \frac{\partial^2 W}{\partial t^2} \quad (16)$$

$$\int_{-\frac{h}{2}}^{\frac{h}{2}} \left[D_z \beta \sin(\beta z) + \frac{\partial D_x}{\partial x} \cos(\beta z) \right] dz = 0 \quad (17)$$

And the boundary conditions are

$$\begin{aligned} \frac{\partial W}{\partial x} &= 0 \text{ or } M = 0 \\ W &= 0 \text{ or } \frac{\partial M}{\partial x} = 0 \\ \frac{\partial W}{\partial x} &= 0 \text{ or } W = 0 \end{aligned} \quad (18)$$

$$\int_{-\frac{h}{2}}^{\frac{h}{2}} D_x \cos(\beta z) dz = 0 \text{ or } \phi = 0$$

In order to determine the bending moment, Eqs. (6) to (8) are integrated over z

$$M - (e_0 a)^2 \frac{\partial^2 M}{\partial x^2} = F_{31} \phi - D_{11} \frac{\partial^2 W}{\partial x^2} \quad (19)$$

$$\int_{-\frac{h}{2}}^{\frac{h}{2}} \left[D_x - (e_0 a)^2 \frac{\partial^2 D_x}{\partial x^2} \right] \cos(\beta z) dz = X_{11} \frac{\partial \phi}{\partial x} \quad (20)$$

$$\begin{aligned} \int_{-\frac{h}{2}}^{\frac{h}{2}} \left[D_z - (e_0 a)^2 \frac{\partial^2 D_z}{\partial z^2} \right] \beta \sin(\beta z) dz \\ = -F_{31} \frac{\partial^2 W}{\partial x^2} - X_{33} \phi \end{aligned} \quad (21)$$

Where

$$\begin{aligned} F_{31} &= \int_{-\frac{h}{2}}^{\frac{h}{2}} e_{31} \beta z \sin(z\beta) dz \\ D_{11} &= \int_{-\frac{h}{2}}^{\frac{h}{2}} C_{11} z^2 dz \end{aligned} \quad (22)$$

$$A_{11} = \int_{-\frac{h}{2}}^{\frac{h}{2}} C_{11} z dz$$

$$X_{11} = \int_{-\frac{h}{2}}^{\frac{h}{2}} \epsilon_{11} [\cos(\beta z)]^2 dz \quad (23)$$

$$X_{33} = \int_{-\frac{h}{2}}^{\frac{h}{2}} \epsilon_{33} [\beta \sin(\beta z)]^2 dz$$

Then, by substituting Eq. (16) into Eq. (19), the bending moment is obtained as

$$M = F_{31} \phi - D_{11} \frac{\partial^2 W}{\partial x^2} + (e_0 a)^2 \left[\rho A \frac{\partial^2 W}{\partial t^2} - N_e \frac{\partial^2 W}{\partial x^2} \right] \quad (24)$$

Therefore, Eq. (16) can be rearranged as

$$\begin{aligned} N_E \frac{\partial^2 W}{\partial x^2} + (F_{31} \frac{\partial^2 \phi}{\partial x^2} - D_{11} \frac{\partial^4 W}{\partial x^4}) \\ + (e_0 a)^2 \left[\rho A \frac{\partial^4 W}{\partial x^2 \partial t^2} - N_e \frac{\partial^4 W}{\partial x^4} \right] \\ = \rho A \frac{\partial^2 W}{\partial t^2} \end{aligned} \quad (25)$$

Because there is not an auxiliary equation that can be used in calculating D_x and D_z , one has to differentiate Eq. (20) with respect to x , first. After that, the terms containing the nonlocal parameter in both Eqs. (20) and (21) have to be neglected. Substituting the two resulting equations in Eq. (17) results in

$$X_{11} \frac{\partial^2 \phi}{\partial x^2} - X_{33} \phi - F_{31} \frac{\partial^2 W}{\partial x^2} = 0 \quad (26)$$

By defining the following non-dimensional parameters

$$\begin{aligned} \xi = \frac{x}{L}, w = \frac{W}{h}, \varphi = \frac{\phi}{\phi_0}, \phi_0 = \sqrt{\frac{A_{11}}{X_{33}}}, \tau = \frac{t}{t_0} \\ t_0 = L \sqrt{\frac{\rho A}{A_{11}}}, \mu = \frac{e_0 a}{L}, \bar{N}_E = \frac{N_E}{A_{11}}, \bar{F}_{31} = \frac{F_{31} \phi_0}{A_{11} h} \\ \bar{D}_{11} = \frac{D_{11}}{L^2 A_{11}}, \bar{X}_{11} = \frac{X_{11} \phi_0^2}{A_{11} h^2}, \bar{X}_{33} = \frac{X_{33} \phi_0^2 L^2}{A_{11} h^2} \end{aligned} \quad (27)$$

Eqs. (25) and (26) can be rearranged in a non-dimensionalized form

$$\begin{aligned} \bar{N}_E \frac{\partial^2 W}{\partial \xi^2} - \bar{D}_{11} \frac{\partial^4 W}{\partial \xi^4} - \mu^2 \bar{N}_E \frac{\partial^4 W}{\partial \xi^4} + \bar{F}_{31} \frac{\partial^2 \varphi}{\partial \xi^2} \\ = \frac{\partial^2 W}{\partial \tau^2} - \mu^2 \frac{\partial^4 W}{\partial \tau^2 \partial \xi^2} \end{aligned} \quad (28)$$

$$\bar{X}_{11} \frac{\partial^2 \varphi}{\partial \xi^2} - \bar{X}_{33} \varphi - \bar{F}_{31} \frac{\partial^2 W}{\partial \xi^2} = 0 \quad (29)$$

The boundary conditions are transformed into

$$w = \frac{\partial \varphi}{\partial \xi} = \frac{\partial w}{\partial \xi} = 0 \quad (30)$$

For the clamped end, and

$$\begin{aligned} M &= -\bar{D}_{11} \frac{\partial^2 W}{\partial \xi^2} + \bar{F}_{31} \varphi + \mu^2 \frac{\partial^2 W}{\partial \tau^2} = 0 \\ \frac{\partial M}{\partial \xi} &= -\bar{D}_{11} \frac{\partial^3 W}{\partial \xi^3} + \bar{F}_{31} \frac{\partial \varphi}{\partial \xi} + \mu^2 \frac{\partial^3 W}{\partial \xi \partial \tau^2} = 0 \\ \phi &= 0 \end{aligned} \quad (31)$$

For the free end of the beam.

3. Solving the equations

3.1 Differential quadrature (DQ) method

In this method, the governing differential equations are transformed into a set of algebraic equations. A detailed introduction on the DQ method can be found in (Shu 2012). By following the algorithm of the DQ method, Eqs. (28) and (29) can be written as

$$\begin{aligned} \bar{N}_E \sum_{m=1}^N c_{im}^2 w_m - \bar{D}_{11} \sum_{m=1}^N c_{im}^4 w_m - \mu^2 \bar{N}_E \sum_{m=1}^N c_{im}^4 w_m \\ + \bar{F}_{31} \sum_{m=1}^N c_{im}^2 \varphi_m = \ddot{w}_i - \mu^2 \sum_{m=1}^N c_{im}^2 \ddot{w}_m, \quad (i=1, \dots, N) \end{aligned} \quad (32)$$

$$\bar{X}_{11} \sum_{m=1}^N c_{im}^2 \varphi_m - \bar{X}_{33} \varphi - \bar{F}_{31} \sum_{m=1}^N c_{im}^2 w_m = 0, \quad (i=1, \dots, N) \quad (33)$$

Where N is the total number of sample points along the beam axis, and c_{im}^k is the m th weighting coefficient of the k th-order differentiation in the i th equation. The boundary conditions of a cantilever beam can also be written as

$$\begin{aligned} w = \sum_{m=1}^N c_{1m}^1 w_m = \sum_{m=1}^N c_{1m}^1 \varphi_m = 0 @ x = 0 \\ \varphi = M = \frac{\partial M}{\partial x} = 0 @ x = L \end{aligned} \quad (34)$$

And for a clamped-clamped beam

$$\begin{aligned} w = \sum_{m=1}^N c_{1m}^1 w_m = \sum_{m=1}^N c_{1m}^1 \varphi_m = 0 @ \xi = 0 \\ w = \sum_{m=1}^N c_{nm}^1 w_m = \sum_{m=1}^N c_{nm}^1 \varphi_m = 0 @ \xi = L \end{aligned} \quad (35)$$

After applying the DQ method to the governing equations and boundary conditions and obtaining the new equations, the displacement vector is defined as

$$d = \left\{ \left\{ w_i \right\}^T, \left\{ \varphi_i \right\}^T \right\}^T \quad i = 1, 2, \dots \quad (36)$$

By defining the displacement vector, the governing equations after applying the DQ method can be written as

$$Kd + M\ddot{d} = 0 \quad (37)$$

After that, the displacement vector is assumed to be

$$d = d e^{i\omega\tau} \quad (38)$$

Where ω is the dimensionless natural frequency and is defined as

$$\omega = \Omega L \sqrt{\frac{\rho A}{A_{11}}} \quad (39)$$

3.2 Galerkin method

In this method, the deflection and electrical potential of the beam are written as the following expansions (Thomsen 2003, Hajnayeb and Khadem 2016)

$$\begin{aligned} w(\xi, \tau) &= \sum_{i=1}^n q_i(\tau) P_i(\xi) \\ \varphi(\xi, \tau) &= \sum_{i=1}^n s_i(\tau) r_i(\xi) \end{aligned} \quad (40)$$

where $P_i(\xi)$ and $r_i(\xi)$ are the admissible functions of the deflection and electric potential of the beam, respectively. $q_i(\tau)$ and $s_i(\tau)$ are the unknown mode participation factors that have to be found. After substituting Eq. (40) into Eq. (29), then multiplying by $P_i(\xi)$ and integrating with respect to ξ over the length of the beam, s_j is obtained with respect to q_i

$$s(j) = \sum_{i=1}^n G_{ji} q_i, \quad j = 1, n \quad (41)$$

where

$$\begin{aligned} G = R^{-1}V, \quad R_{ji} = \int_0^1 [\bar{X}_{11} P_j r_i'' - \bar{X}_{11} P_j r_i] d\xi, \\ V_{ji} = \int_0^1 [\bar{F}_{31} P_j P_i'] d\xi \end{aligned} \quad (42)$$

Then, substituting Eqs. (40) and (42) into Eq. (28), and then multiplying by $P_i(\xi)$ and integrating with respect to ξ over the length of the beam result in

$$N_{ji} \ddot{q}_i + Q_{ji} q_i = 0, \quad i = 1, n, \quad j = 1, n \quad (43)$$

where N_{ji} and Q_{ji} are

$$\begin{aligned} N_{ji} &= \int_0^1 P_j P_i d\xi - \int_0^1 \mu^2 P_j P_i' d\xi \\ Q_{ji} &= \int_0^1 P_j \bar{D}_{11} P_i''' d\xi - \int_0^1 P_j \bar{F}_{31} G_{ij} r_i'' d\xi \\ &\quad - \int_0^1 \bar{N}_E P_j P_i' d\xi + \mu^2 \int_0^1 \bar{N}_E P_j P_i''' d\xi \end{aligned} \quad (44)$$

In order to obtaining natural frequencies, following eigen value problem must be solved

$$(N^{-1}Q - \bar{\omega}_n^2 I)q = 0 \quad (46)$$

Where $\bar{\omega}_n$ is the natural frequency of the beam. The mode shapes of both cantilever and clamped-clamped (C-C) beams have the following form (Inman and Singh 2001)

Table 1 the values of β_i for a cantilever and a C-C beam

Mode no.	Cantilever	Clamped-Clamped
1	1.8751	4.7300
2	4.6940	7.8532
3	7.8548	10.9956

$$P_i(\xi) = \cosh \beta_i \xi - \cos \beta_i \xi - \sigma_i (\sinh \beta_i \xi - \sin \beta_i \xi) \quad (47)$$

where, for a cantilever beam, the values of σ_i are defined as

$$\sigma_i = \frac{\sinh \beta_i - \sin \beta_i}{\cosh \beta_i + \cos \beta_i} \quad (48)$$

and β_i are the roots of the following equation

$$\cosh \beta_i \cos \beta_i = -1 \quad (49)$$

For a C-C beam, the values of σ_i and β_i can be obtained from

$$\sigma_i = \frac{\cosh \beta_i - \cos \beta_i}{\sinh \beta_i - \sin \beta_i} \quad (50)$$

and

$$\cosh \beta_i \cos \beta_i = 1 \quad (51)$$

The values of β_i for the first three modes of a beam are written in Table 1. These mode shapes are used as the admissible functions, $P_i(\xi)$, of the piezoelectric beam in this study.

The n th electrical potential admissible function for a cantilever beam, $r_i(\xi)$, is defined as

$$r_i(\xi) = \cos \left[\left(\frac{2i-1}{2} \right) \pi \xi \right] \quad (52)$$

and

$$r_i(\xi) = \cos \left[(i+1) \pi \xi \right] \quad (53)$$

For a clamped-clamped beam, in order that they satisfy the boundary conditions of the system.

4. Numerical results

As mentioned before, Ke *et al.* (2012) used Timoshenko beam theory to study the vibrations of a piezoelectric Nanobeam. In order to compare the results of the current study with their results, the derivation of equations and solution algorithms are also implemented based on Timoshenko theory. Moreover, the dimensions and material properties of the beam are considered the same as this reference.

The natural frequencies of the first three modes are compared in Table 2. The first natural frequencies are in good agreement, however comparing the natural frequencies for the second and third modes shows a significant difference.

Next, the results of solving the equations for a numerical example are presented. The piezoelectric beam is assumed

Table 2 comparing the natural frequencies of the first three mode shapes obtained in this paper with the results of (Ke 2012) ($\mu=0$, $V_0=0$, $L=80$ nm, $h=10$ nm)

Mode no	This research (Timoshenko)	(Ke 2012) [GHz]	Difference (%)
1	5.7351	5.7266	0.15
2	13.7465	27.3155	49.66
3	23.8466	47.0167	49.28

Table 3 material properties of PZT-4 (Wang 2002b)

c_{11} (GPa)	132
e_{31} (Cm ⁻²)	-4.1
ϵ_{11} (Cv ⁻¹ m ⁻¹)	5.841×10^{-9}
ϵ_{33} (Cv ⁻¹ m ⁻¹)	7.124×10^{-9}
ρ (Kg m ⁻³)	7500

Table 4 convergence study of natural frequencies (GHZ) ($L/h=30$)

no. of accuracy points	1st natural frequency [GHz]	
	Cantilever	C-C
6	0.05088	0.37541
8	0.05065	0.32349
10	0.05064	0.32236
14	0.05066	0.32235
17	0.05066	0.32235
22	0.05066	0.32235
27	0.05066	0.32235

Table 5 comparing the natural frequencies of the first three mode shapes of the C-C Nanobeam based on Timoshenko and Euler-Bernoulli beam theory ($\mu=0$, $V_0=0$, $L=450$ nm, $h=15$ nm)

Mode no.	This study (Timoshenko) [GHz]	This study (Euler-Bernoulli) [GHz]	Difference (%)
1	0.3174	0.3220	1.43
2	0.8605	0.8877	3.06
3	1.6521	1.7402	5.06

to be made of PZT-4 with mechanical and electrical properties listed in Table 3. In this example, the beam is 300nm long with the thickness of 15nm.

Table 4 shows the results of the convergence study of the first natural frequency. The results show that the response of the C-C beam converges faster than the cantilever beam.

Then, the first three vibration modes of a beam with a high aspect ratio ($\frac{L}{h} = 30$), are calculated using both of Euler-Bernoulli and Timoshenko theories. The results are presented in Table 5. As expected, the results are the same for both theories because of the high aspect ratio of the beam.

The first and second dimensionless natural frequencies of the studied C-C and cantilever beams are presented in Tables 6 and 7, respectively.

Table 6 natural frequencies (GHZ) of the first two mode shapes of the C-C Nanobeam for different values of the nonlocal parameter ($V_0=0$)

μ	1st mode			2nd mode		
	Galerkin	DQ	Difference [%]	Galerkin	DQ	Difference [%]
0	0.32212	0.32235	0.07	0.88859	0.88854	0.01
0.1	0.30392	0.30413	0.07	0.73472	0.73449	0.03
0.2	0.26334	0.26350	0.06	0.52519	0.52471	0.09
0.3	0.22108	0.22119	0.05	0.38946	0.38896	0.13

Table 7 natural frequencies (GHZ) of the first two mode shapes of the cantilever Nanobeam for different values of the nonlocal parameter ($V_0=0$)

μ	1st mode			2nd mode		
	Galerkin	DQ	Difference [%]	Galerkin	DQ	Difference [%]
0	0.05007	0.05066	1.16	0.31520	0.31754	0.74
0.1	0.05029	0.05037	0.16	0.29586	0.29521	0.22
0.2	0.05098	0.05156	1.12	0.25153	0.25316	0.64
0.3	0.05225	0.05283	1.1	0.20302	0.20429	0.62

Table 8 natural frequencies (GHZ) of the first two modes of a C-C beam for different values of external voltage and ($\mu=0$)

V_0	1st mode			2nd mode		
	Galerkin	DQ	Difference [%]	Galerkin	DQ	Difference [%]
0.6	0.37035	0.37056	0.06	0.95668	0.95664	0.00
0.2	0.33904	0.33927	0.07	0.91188	0.91185	0.00
0	0.32212	0.32235	0.07	0.88859	0.88854	0.01
-0.2	0.30417	0.30440	0.07	0.86462	0.86456	0.01
-0.6	0.26425	0.26449	0.09	0.81446	0.81432	0.02

The results are obtained from both Galerkin and DQ methods, which show a negligible differences. The difference between the results of these two methods is not significant because the applied admissible functions in Galerkin method are quite close to the actual mode shapes of the system. This closeness stems mostly from the simple geometry of the studied system. The results also present that an increase in the nonlocal parameter, μ , decreases the beam natural frequencies, except for the first mode shape of a cantilever beam. On the contrary, the first natural frequency of a cantilever beam increases slightly by increasing the nonlocal parameter. Lu *et al* (2006) reported the same finding.

The effect of applying a voltage to the C-C beam is presented in Table 8, where a negative voltage decreases the natural frequencies, and a positive voltage increases them. This behavior is because of the resulting axial force from applying the voltage, which changes the stiffness of the system. The natural frequencies obtained from Galerkin and DQ methods are in good agreement.

The electric potential mode shape in the C-C and cantilever beams for different values of the nonlocal parameter are depicted in Figs. 2 and 3, respectively. It is

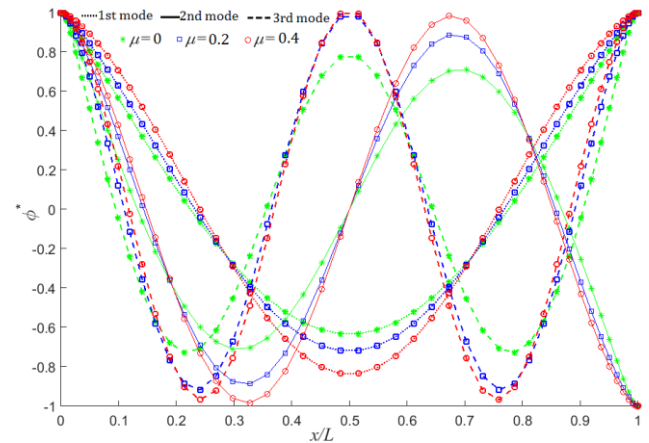


Fig. 2 the electric potential mode shapes of the C-C nanobeam for different values of the nonlocal parameter and $V_0=0$

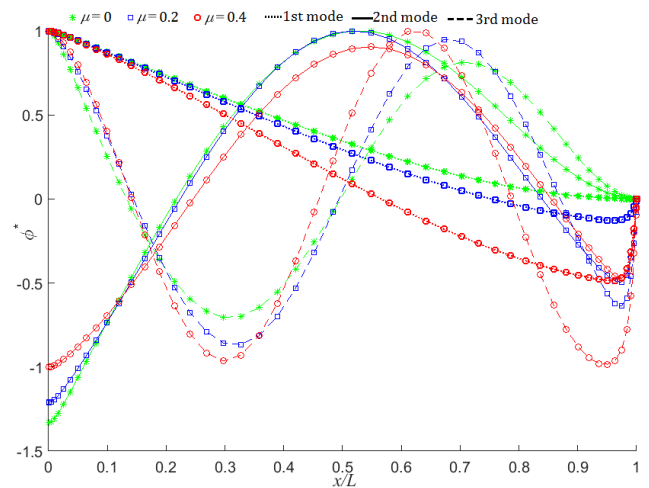


Fig. 3 the electric potential mode shapes of the cantilever nanobeam for different values of the nonlocal parameter and $V_0=0$

observed that the maximums are located at the points where the value of stress is maximum because of piezoelectric properties of the beam.

For both kinds of B.C.s, the maximums of electric potential mode shapes are located close to the clamped ends. In contrast, the amplitudes of the potential mode shapes decrease at locations close to the free ends. It can also be observed that higher mode shapes are affected more significantly by the changes in the nonlocal parameter. Similar results are observed in Tables 5 and 6 that confirm the higher sensitivities of the higher modes to the magnitude of the nonlocal parameter. The vibration mode shapes of a C-C and a cantilever beam are shown in Figs. 4 and 5.

Fig. 4 shows that the nonlocal parameter has negligible effects on the first two modes of a C-C beam, while the third mode is significantly affected by this parameter. Fig. 5 depicts the significant effects of the nonlocal parameter on the three modes of a cantilever beam. These effects are significant for higher modes.

The effect of external voltage on the electric potential

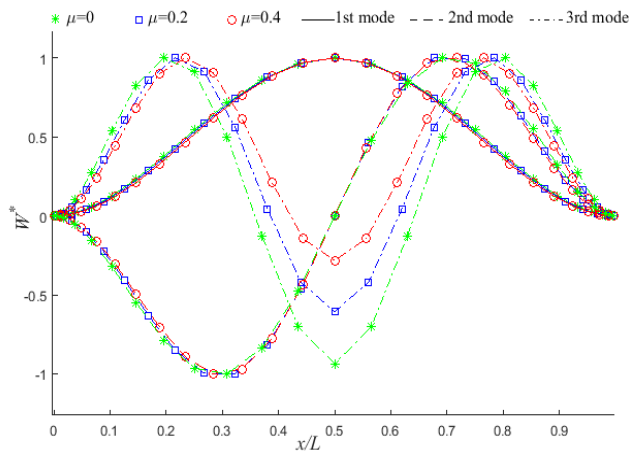


Fig. 4 The vibration mode shapes of the C-C nanobeam for different values of the nonlocal parameter and $V_0=0$

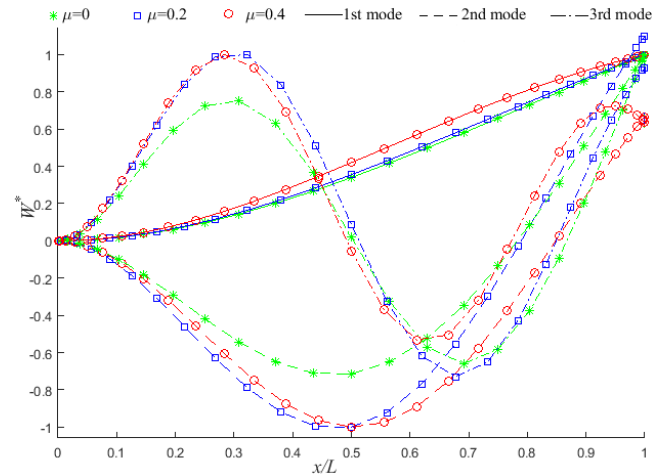


Fig. 5 The vibration mode shapes of the cantilever nanobeam for different values of the nonlocal parameter and $V_0=0$

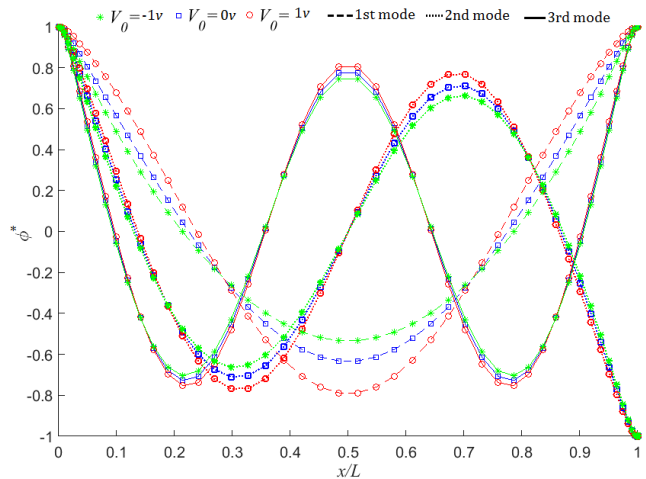


Fig. 6 The electric potential mode shapes of the C-C nanobeam for different values of the applied voltage

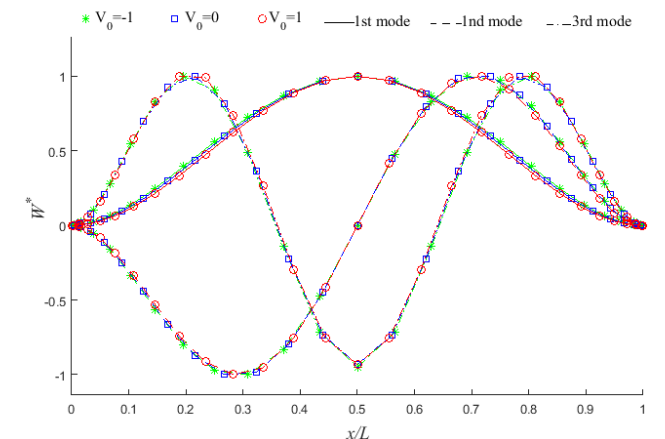


Fig. 7 The vibration mode shapes of the C-C nanobeam for different values of the applied voltage

and vibration mode shapes of the C-C beam are shown in Figs. 6 and 7. It is observed that the effect of the applied voltages on the potential mode shapes is more significant. In contrast, the vibration mode shapes are independent of the applied voltage.

The effect of external voltage on the electric potential and vibration mode shapes of the C-C beam are shown in Figs. 6 and 7. It is observed that the effect of the applied voltages on the potential mode shapes is more significant. In contrast, the vibration mode shapes are independent of the applied voltage.

The applied methods of Galerkin and DQ have pros and cons. First, Galerkin method is not able to find the mode shapes of the system while DQ gives the mode shapes of both vibrations and generated voltage of the piezoelectric beam. The algorithm of Galerkin method is significantly simpler comparing to DQ but has higher error levels in complex nonlinear systems. Therefore, for complex piezoelectric systems DQ method can be used for obtaining the mode shapes. If a change in the model is encountered, these mode shapes are applicable in Galerkin method for a fast analysis of the new system.

7. Conclusions

This paper studies the free vibrations of a piezoelectric nanobeam for different values of the nonlocal parameter. The nonlocal elasticity and Euler-Bernoulli beam theory are used to model the nanobeam. The equation of motion and boundary conditions are derived by using Hamilton's principle. The obtained equations are then solved by using the DQ and Galerkin method. The difference between the results of these two methods was negligible that shows the applicability and success of Galerkin method. The results also show that an increase in the nonlocal parameter increases the beam natural frequencies. Moreover, increasing the applied positive voltage increases the axial force and therefore natural frequencies of the system. The same fact is observed by decreasing the applied negative voltage. Finally, it was found that the maximums of the electric potential mode shapes are located at the points where the induced mechanical stresses in the vibration mode shape of the beam are maximum.

Acknowledgments

The research described in this paper was financially supported by Shahid Chamran University of Ahvaz.

References

- Erturk, A. and Inman, D.J. (2011), *Piezoelectric Energy Harvesting*, John Wiley & Sons.
- Gautschi, D. (2002), *Piezoelectric Sensors*, Springer, New York, USA.
- Hajnayeb, A. and Khadem, S.E. (2015). "An analytical study on the nonlinear vibration of a double-walled carbon nanotube", *Struct. Eng. Mech.*, **54**(5), 987-998.
- Hosseini-Hashemi, S., Nahas, I., Fakher, M. and Nazemnezhad, R. (2014), "Surface effects on free vibration of piezoelectric functionally graded nanobeams using nonlocal elasticity", *Acta Mechanica*, **225**(6), 1555-1564 .
- Inman, D.J. and Singh, R.C. (2001), *Engineering Vibration*, Prentice Hall Upper Saddle River.
- Jalili, N. (2009), *Piezoelectric-Based Vibration Control: From Macro To Micro/Nano Scale Systems*, Springer Science & Business Media, boston, USA.
- Junwu, K., Zhigang, Y., Taijiang, P., Guangming, C. and Boda, W. (2005), "Design and test of a high-performance piezoelectric micropump for drug delivery", *Sens. Actuat. A: Phys.*, **121**(1), 156-161.
- Ke, L.L. and Wang, Y.S. (2012), "Thermoelectric-mechanical vibration of piezoelectric nanobeams based on the nonlocal theory", *Smart Mater. Struct.*, **21**(2), ID 025018.
- Ke, L.L., Wang, Y.S. and Wang, Z.D. (2012), "Nonlinear vibration of the piezoelectric nanobeams based on the nonlocal theory", *Compos. Struct.*, **94**(6), 2038-2047.
- Koh, K.H., Kobayashi, T., Hsiao, F.L. and Lee, C. (2010), "Characterization of piezoelectric PZT beam actuators for driving 2D scanning micromirrors", *Sens. Actuat. A: Phys.*, **162**(2), 336-347.
- Lu, P., Lee, H., Lu, C. and Zhang P. (2006), "Dynamic properties of flexural beams using a nonlocal elasticity model", *J. Appl. Phys.*, **99**(7), ID 073510.
- Shu, C. (2012), *Differential Quadrature And its Application In Engineering*, Springer Science & Business Media, London.
- Song, G., Sethi, V. and Li, H.N. (2006), "Vibration control of civil structures using piezoceramic", *Smart Mater.*, **28**(11), 1513-1524.
- Thomsen, J.J. (2003), *Vibrations And Stability: Advanced Theory, Analysis, And Tools*, Springer Science & Business Media, Denmark.
- Uchino, K. (1997), *Piezoelectric Actuators and Ultrasonic Motors*, Springer Science & Business Media, Boston, USA.
- Wang, Q. (2002a), "Axi-symmetric wave propagation in a cylinder coated with a piezoelectric layer", *Int. J. Solid. Struct.*, **39**(11), 3023-3037.
- Wang, Q. (2002b), "On buckling of column structures with a pair of piezoelectric layers", *Eng. Struct.*, **24**(2), 199-205.
- Zamanian, M. and Khadem, S.E. (2009), "Nonlinear vibration of an electrically actuated microresonator tuned by combined DC piezoelectric and electric actuations", *Smart Mater. Struct.*, **19**(1), 015012.
- Zhang, J., Wang, C. and Bowen, C. (2014), "Piezoelectric effects and electromechanical theories at the nanoscale", *Nanoscale*, **6**(22), 13314-13327.